Development and characterization of composite materials with multi-walled carbon nanotubes and graphene nanoplatelets for powder bed fusion

Ana C. Lopes
IPC – Institute for Polymers and Composites, University of Minho, Guimarães, Portugal and DONE Lab – Advanced Manufacturing of Products and Tools, University of Minho, Guimarães, Portugal
Álvaro M. Sampaio
IPC – Institute for Polymers and Composites, University of Minho, Guimarães, Portugal; DONE Lab – Advanced Manufacturing of Products and Tools, University of Minho, Guimarães, Portugal and Lab2PT, School of Architecture, University of Minho, Guimarães, Portugal, and
António J. Pontes
IPC – Institute for Polymers and Composites, University of Minho, Guimarães, Portugal and DONE Lab – Advanced Manufacturing of Products and Tools, University of Minho, Guimarães, Portugal

Abstract

Purpose – With the technological progress, high-performance materials are emerging in the market of additive manufacturing to comply with the advanced requirements demanded for technical applications. In selective laser sintering (SLS), innovative powder materials integrating conductive reinforcements are attracting much interest within academic and industrial communities as promising alternatives to common engineering thermoplastics. However, the practical implementation of functional materials is limited by the extensive list of conditions required for a successful laser-sintering process, related to the morphology, powder size and shape, heat resistance, melt viscosity and others. The purpose of this study is to explore composite materials of polyamide 12 (PA12) incorporating multi-walled carbon nanotubes (MWCNT) and graphene nanoplatelets (GNP), aiming to understand their suitability for advanced SLS applications.

Design/methodology/approach – PA12-MWCNT and PA12-GNP materials were blended through a pre-optimized process of mechanical mixing with various percentages of reinforcement between 0.50 wt.% and 3.00 wt.% and processed by SLS with appropriate volume energy density. Several test specimens were produced and characterized with regard to processability, thermal, mechanical, electrical and morphological properties. Finally, a comparative analysis of the performance of both carbon-based materials was performed.

Findings – The results of this research demonstrated easier processability and higher tensile strength and impact resistance for composites incorporating MWCNT but higher tensile elastic modulus, compressive strength and microstructural homogeneity for GNP-based materials. Despite the decrease in mechanical properties, valuable results of electrical conductivity were obtained with both carbon solutions until 10^{-6} S/cm.

Originality/value – The carbon-based composites developed in this research allow for the expansion of the applicability of laser-sintered parts to advanced fields, including electronics-related industries that require functional materials capable of protecting sensitive devices against electrostatic discharge.

Keywords Additive manufacturing, Selective laser sintering, Composite materials, Polyamide 12, MWCNT, GNP

Paper type Research paper

1. Introduction

Selective laser sintering (SLS) is a powder bed fusion technology wherein polymeric parts are produced through powder material that is fused by the thermal energy of a laser source according to a previously sliced computer-aided design model (ASTM, 2012; Lopes *et al.*, 2022b). For processing, conventional laser-sintering systems comprise:

- a closed chamber for thermal and atmospheric control;
- powder bins for material feeding;
- a recoater for powder dosing and dispensing;
- a building platform for the layer-by-layer manufacturing; and

The current issue and full text archive of this journal is available on Emerald Insight at: **https://www.emerald.com/insight/1355-2546.htm**

Rapid Prototyping Journal

[DOI 10.1108/RPJ-04-2023-0142]

This research was co-funded by the European Regional Development Fund through the Operational Competitiveness and Internationalization Programme (COMPETE 2020) [Project No. 47108, "SIFA"; Funding Reference: POCI-01-0247-FEDER-047108] and by the Foundation for Science and Technology (FCT) through the PhD scholarship 2020.04520.BD.

Conflicts of interest: The authors have no conflicts of interest to declare.

Received 18 April 2023
Revised 8 August 2023
Accepted 5 September 2023

- an optical system including the laser source and scanning mirrors (Figure 1).

Since its development, SLS has undergone significant technological progress in terms of control systems and materials, which in recent years has led to attractive compound annual growth rates (e.g. projection of 12.9% from 2022 to 2028) (MarketWatch, 2022). The promising capability of SLS for the manufacturing of end-use parts has propelled scientific research focused on the development of composite materials with novel functionalities for advanced technical applications as an alternative to conventional polyamides (Yuan *et al.*, 2019). Of all possibilities, materials incorporating carbon-based particles are being extensively studied, aiming for the production of laser-sintered parts with improved mechanical, thermal and electrical performance (Francis and Jain, 2015; Salmoria *et al.*, 2017; Wu *et al.*, 2020). In turn, carbon-based particles have different potential to improve mechanical and electrical properties depending on the type of hybridization which defines their structural rearrangement and microstructure (Ma-Hock *et al.*, 2013; Asadi and Kalaitzidou, 2018; Kharisov and Kharissova, 2019; Razeghi, 2019). Graphene and multi-walled carbon nanotubes (MWCNT) are two different forms of carbon, known as carbon allotropes, broadly studied. Graphene is a two-dimensional monolayer of carbon atoms arranged in a hexagonal network which is obtained from the exfoliation of graphite (Ferreira, 2013; Ma-Hock *et al.*, 2013; Asadi and Kalaitzidou, 2018; Kharisov and Kharissova, 2019). MWCNT are two or more concentric cylinders of graphene sheets with diameters ranging between 1.4 and 100 nm (Ferreira, 2013; Ma-Hock *et al.*, 2013; Asadi and Kalaitzidou, 2018). Despite the similar performance of both carbon-based particles, the differences in the structural rearrangement allow graphene to surpass the properties of carbon nanotubes in various applications (Zakaria *et al.*, 2017; Sanivada *et al.*, 2022). Because of that, and due to the high cost of graphene, promising cost-effective alternatives have become available, such as graphene nanoplatelets (GNP) (Sanivada *et al.*, 2022). Both MWCNT and GNP are widely used to reinforce polymer materials with the aim of modifying and/or improving the properties of polymers processed by conventional and/or non-conventional processing methods, such as additive manufacturing (Madhad *et al.*, 2021; Lopes *et al.*, 2022a).

Figure 1 Schematics of SLS process

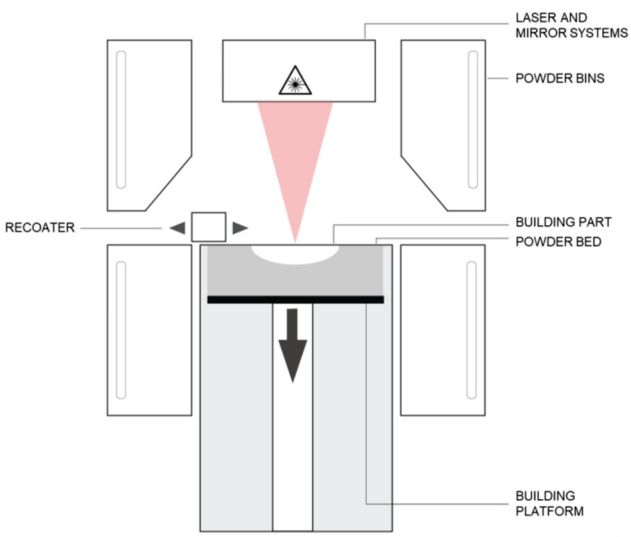

Source: Figure by authors

MWCNT are widely considered in the development of composite materials for SLS, using the most common PA12 material as polymer matrix. Through the simplest method of mechanical mixing, Salmoria *et al.* (2011, 2017) developed composite materials of PA12 incorporating 0.5 wt.%, 1.0 wt.% and 3.0 wt.% of MWCNT. In their studies, improvements in mechanical and electrical properties in relation to the polymer matrix were reported until a high critical amount of incorporation, where the electrical properties increased with the decrease of the mechanical ones. Bai *et al.* (2013, 2014, 2015) used a specific coating method to produce composite parts with PA12 incorporating 0.1 wt.% and 0.2 wt.% of MWCNT. Besides the improvements in mechanical properties, advantages in thermal properties were also observed, namely, with regard to thermal conductivity. Paggi *et al.* (2013) developed composite materials of PA12 incorporating 0.5 wt.%, 1.0 wt.% and 3.0 wt.% of MWCNT through magnetic stirring of solutions and mechanical mixing. They proved the influence of the processing parameters, namely, the laser power and scan speed, on the manufacturing of quality parts. Through precipitation of solutions, Yuan *et al.* (2016, 2018) incorporated 0.1 wt.%, 0.5 wt.% and 1.0 wt.% of MWCNT pre-modified with sodium cholate into a PA12 matrix. Benefits in tensile strength and electrical and thermal conductivity were achieved.

Despite the outstanding properties of graphene, there are fewer publications exploring its incorporation in polyamide-base matrices for powder bed fusion processes. Makuch *et al.* (2015) evaluated PA12 with 1.0 wt.% of graphene flakes mechanically mixed for 1 h, 2 h, 4 h and 8 h. The results proved the influence of the mixing time on the dispersion of the reinforcement and its interfacial adhesion with the matrix, with the highest value being more advantageous for the sintering. De Leon *et al.* (2018) evaluated PA12 with graphene oxide in the volume percentages of 0.12 vol%, 0.18 vol%, 0.36 vol% and 0.72 vol% prepared through precipitation of solutions after an exfoliation process. Composite parts with 0.36 vol% graphene oxide presented an elastic modulus 48% higher than neat-PA12 parts with similar tensile strength. Based on statistical analyses, the electrical percolation threshold was defined for 0.05 vol% of incorporation.

In addition to the typology and amount of incorporation, the influence of the carbon-based reinforcements on the properties of SLS parts depends on the process parameters, namely, the energy density which is defined by the layer thickness, laser power, scan speed and hatch distance (Lopes *et al.*, 2022a). When the energy input to the powder particles increases, the porosity of parts decreases and the density and mechanical properties increase until degradation begins (Czelusniak and Amorim, 2020; Tong *et al.*, 2020). For PA12, values between 0.158 and 0.238 J/mm^3 are adequate for dimensional and geometric properties and values between 0.278 and 0.318 J/mm^3 for mechanical strength (Lopes *et al.*, 2022b). In turn, the processing of carbon-based composite materials requires specific adjustment of the sintering variables, as this type of reinforcement intensifies the conduction of the energy supplied by the laser beam through the layers of powder

compared to conventional thermoplastics such as polyamides (Salmoria *et al.*, 2011; Bai *et al.*, 2013, 2015). Prior optimization of the main SLS process parameters is therefore an essential condition to avoid warpage and curling effects and to maximize the density and mechanical strength of the parts produced, depending on the reinforcement (Eshraghi *et al.*, 2013; Paggi *et al.*, 2013; Tian *et al.*, 2018; Hong *et al.*, 2019). Nevertheless, even with critical control of the operating variables, ensuring a stable sintering process and quality interparticle adhesion without agglomeration and/or porosity at reasonable development cost are difficulties widely reported in literature (Parandoush and Lin, 2017; Asadi and Kalaitzidou, 2018; Madhad *et al.*, 2021; Lopes *et al.*, 2022a).

Despite the increasing number of scientific publications in recent years, to the best of the authors' knowledge, there is not any research that directly compares composite materials incorporating different carbon-based reinforcements under the same conditions of development, evaluating their suitability for SLS. Hence, this research investigates composite materials of a PA12 powder incorporating MWCNT and GNP, without pre-treatment or modification, in the weight percentages of 0.50 wt.%, 1.75 wt.% and 3.00 wt.%. The composite materials were prepared via mechanical mixing for 12 h at room temperature and processed in a commercial laser-sintering machine with pre-optimized volume energy density. The macro- and micro-scale properties of the developed composites were assessed through thermal, mechanical, electrical and morphological characterization tests. Data from a previously published study was considered for this analysis (Lopes *et al.*, 2022a). The main targets of this research include understanding the potentialities and limitations of composite materials incorporating carbon-based reinforcements with regard to SLS processability and properties of parts produced through a comparative analysis.

2. Materials and methods

In this study, PA 2200 from EOS GmbH in a mixture ratio of 1:1 (virgin and processed) was used as PA12 matrix, and MWCNT NC7000^{TM} from NANOCYL and GNP from Graphenest, S.A. were used in the weight percentages of 0.50 wt.%, 1.75 wt.% and 3.00 wt.% as carbon-based reinforcements. The composite materials were prepared through mechanical mixing at 15 revolutions per minute for 12 h at room temperature. After preparation, the blended mixture was processed in an EOS P 396 laser-sintering machine containing vibrating powder dispensers operating at 10–15 L/min of fluidisation flow rate to minimize compaction effects. The samples were produced with the medium-low energy value of 0.238 J/mm^3 defined after a prior optimization for the conditions of the study by proper definition of the layer thickness, laser power, scan speed and hatch distance (Table 1).

Experiments with neat PA12 material were carried out for reference. Several test specimens were positioned in the XYZ orientation in the centre of the building platform to guarantee accurate thermal stability during processing. Blasting and polishing stations were considered to clean the test specimens in post-production operations. Hereafter, the powder composite materials were characterized by differential scanning calorimetry (DSC) in a Netzsch DSC 200 F3 Maia according to ISO 11357 to determine their melting and crystallization temperatures, which define the thermal processing window for SLS. A small portion of the sample was analysed under a nitrogen atmosphere in a first heating from 30°C to 230°C, cooling from 230°C to 30°C, and second heating from 30°C to 230°C. The produced test specimens were then characterized in terms of surface roughness using an InfiniteFocusSL Alicona microscope operating at 10× objective magnification with lateral topographic resolution of 2 μm. An Instron 5969 Universal Testing System was used to carry out tensile tests at 1 mm/min (ISO 527–2) and compression tests at 1.3 mm/min (ASTM D695) using a load cell of 50 kN at room temperature. V-notch Izod impact tests were performed in a CEAST Impact Testing Machine at room temperature according to the Test Method A of ASTM D256, using a pendulum with 4 J of capacity. The electrical properties were assessed through surface measurements on flat plates using a Keithley Model 8009 Resistivity Test Fixture operating at 10 V (ASTM D257). Finally, the microstructure of the composite materials previously prepared with 15 nm of gold coating was evaluated by scanning electron microscopy (SEM) in a Nano SEM FEI Nova 200.

Table 1 SLS Process parameters

Hatching	
Laser power (W)	32
Scan speed (mm/s)	3,730
Hatch distance (mm)	0.30
Extra beam offset (mm)	0.12
Contour and post contour	
Scan speed (mm/s)	3,000
Laser power (W)	34
Extra beam offset (mm)	0
Layer thickness (mm)	0.12
Process chamber temperature (°C)	173
Removal chamber temperature (°C)	130
Beam offset (mm)	0.32

Source: Table by authors

3. Results and discussion

3.1 Preparation and processing characteristics

In the initial development stages, it was verified that weight percentages of incorporation of MWCNT and GNP beyond a high critical value prevent the preparation of homogeneous and consistent powder mixtures. Regarding MWCNT, agglomerates and particles migrated to the borders were observed during the mechanical mixing, in particular for composites incorporating 3.00 wt.% of reinforcement (Figure 2). In turn, despite the potential of GNP to promote greater dispersions after long periods of mixing, the inclusion of this reinforcement in the mixture resulted in a final material with a high level of compaction, with several particles that stuck together, compromising the powder flowability (Figure 3).

Owing to the significant powder compaction effects, composites incorporating GNP were more difficult to process than PA12 and PA12-MWCNT materials. Regarding the processing parameters, it was verified that as the amount of MWCNT and GNP increases in the mixture, lower values of energy density are required for the sintering, as such reinforcements intensify the conduction of energy through the layers of powder.

Figure 2 Agglomeration of MWCNT during mechanical mixing

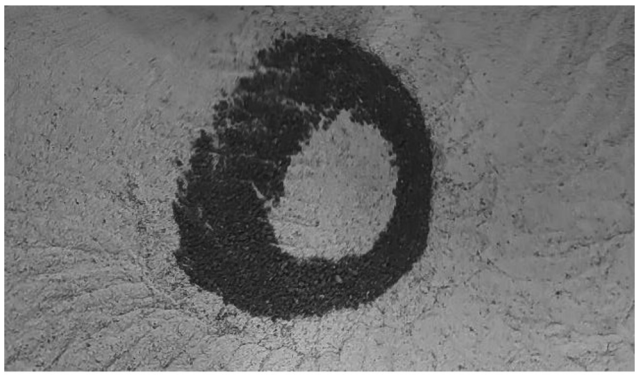

Source: Figure by authors

Once the process was optimized, the composite parts were successfully produced with 0.238 J/mm^3 of volume energy density. Primary observations evidenced darker colouring with the increasing weight percentage of incorporation of reinforcements. Regardless of the colour, visual and tactile perceptions suggested smoother surface finishing for test specimens produced with PA12-GNP materials (Figure 4). Rougher surfaces, as observed in test specimens produced with PA12-MWCNT materials, required more intensive cleaning steps.

3.2 Surface roughness

In a previous published work (Lopes *et al.*, 2022a), it was demonstrated that the surface roughness of test specimens produced with PA12-MWCNT materials increased by ~19% with the incorporation of reinforcement from 0.50 wt.% to 3.00 wt.%. In test specimens produced with PA12-GNP materials, a significant influence of the increasing amount of GNP on the surface topography of the test specimens was also observed (Figure 5).

The test specimens produced with PA12 incorporating 0.50 wt.%, 1.75 wt.% and 3.00 wt.% of GNP presented values of arithmetic mean height (Sa) of 16.3 μm, 16.9 μm and 17.7 μm, respectively, on their upward-facing surfaces in a rising trend. This represents an average increase of ~9% with the incorporation of GNP from 0.50 wt.% to 3.00 wt.%. Although the Sa values cannot be directly compared to those obtained for PA12-MWCNT [the experimental parameters (e.g. exposure time, contrast and resolution) were differently adjusted to each surface topography], the variation in PA12-GNP is smaller than that recorded in PA12-MWCNT materials. This result indicates that the surface roughness of laser-sintered parts is more influenced by the incorporation of MWCNT than GNP, which agrees with the characteristics of surface finishing shown in Figure 4.

3.3 Thermal properties

The DSC thermograms obtained for PA12, PA12-MWCNT and PA12-GNP materials are shown in Figure 6. In all of them, it is possible to evidence a single endothermic peak of fusion and exothermic peak of crystallization, respectively, detected during the heating and cooling of the samples.

Based on the corresponding DSC thermograms, the thermal processing window of the developed materials was identified with the upper and lower limits, respectively, defined by their melting and crystallization temperatures (Figure 7). The operating window of PA12 between 145°C and 177°C (i.e. thermal interval of 32°C) was considered a reference.

In the DSC thermograms, no significant modifications were observed in the melting temperature, which recorded values

Figure 3 Mechanical mixing of PA12-GNP materials in initial (left) and final (right) stages

Source: Figure by authors

Figure 4 Surface of test specimens produced by SLS with PA12 incorporating 3.00 wt.% of MWCNT (left) and 3.00 wt.% of GNP (right)

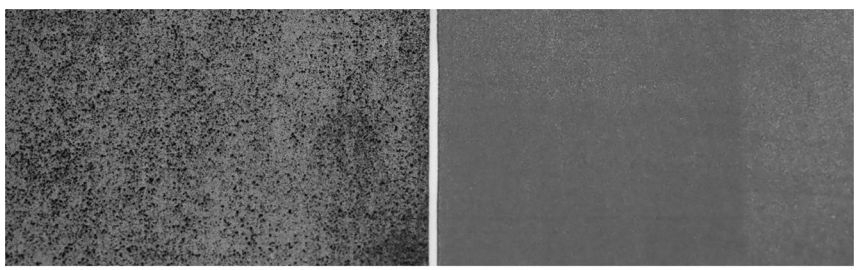

Source: Figure by authors

Figure 5 Surface topography of test specimens produced by SLS with PA12 incorporating 0.50 wt.% (top), 1.75 wt.% (middle) and 3.00 wt.% (bottom) of GNP

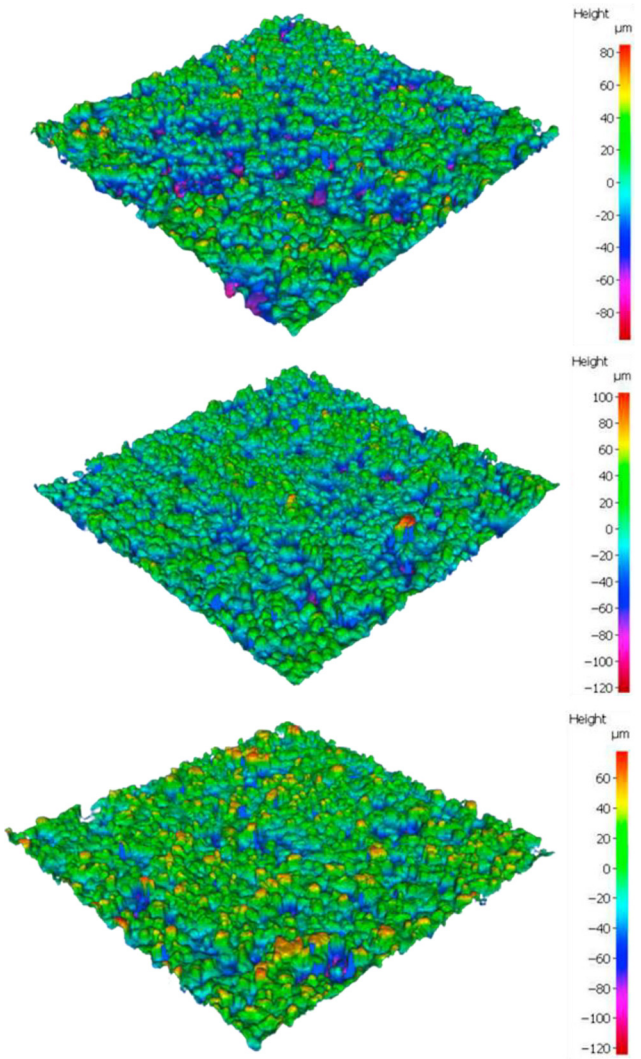

Source: Figure by authors

close to 177°C in all materials. On the other hand, the results showed that the incorporation of MWCNT and GNP increased the crystallization temperature of the base material to 151°C and 150°C (on average), respectively. This suggests that the carbon-based reinforcements acted as nucleating agents, influencing the crystallinity of PA12. In consequence, PA12-MWCNT and PA12-GNP materials presented a thermal processing window 6°C and 5°C narrower than the base matrix, respectively. Compared to PA12, the degree of crystallinity of PA12-MWCNT was not significantly modified, but it slightly increased (~ 2%) with the incorporation of GNP.

3.4 Mechanical properties

The influence of the incorporation of carbon-based reinforcements on the mechanical performance of laser-sintered parts under tensile, compressive and impact loads is discussed in this section.

The stress–strain curves obtained from the tensile tests revealed the significant influence of MWCNT and GNP on the properties of PA12. Regardless of the type of reinforcement and weight percentage of incorporation, the elastic modulus and tensile strength of the resulting composites decreased in relation to the matrix (Figure 8). From 0.50 wt.% to 3.00 wt.%, the elastic modulus decreased 25.9% in PA12-MWCNT materials and 18.6% in PA12-GNP materials, reaching minimum values of 1,088.0 ± 19.6 MPa and 1,295.1 ± 74.2 MPa, respectively. In all conditions, composite materials incorporating GNP presented higher elastic modulus than composites incorporating MWCNT, which may be related to the higher crystallinity rate induced by the incorporation of GNP. In relation to tensile strength, although PA12-MWCNT materials presented higher values than PA12-GNP materials, they exhibited a decrease of 40.1% until 3.00 wt.%, exceeding the decrease of 34.9% in materials incorporating GNP. Compared to the reference value of 45.0 MPa in PA12 test specimens, minimum values close to 22 MPa were obtained with the incorporation of these carbon-based reinforcements.

Similar results were observed for compression properties (Figure 9). In general, PA12-GNP materials revealed greater compressive modulus and compressive strength than PA12-MWCNT materials, despite the decrease in relation to the neat-PA12 matrix. In this regard, values of compressive modulus of 1,454.3 ± 24.2 MPa and 1,141.2 ± 25.5 MPa were recorded in composites incorporating 0.50 wt.% and 3.00 wt.% of GNP, respectively, with compressive strength of 47.6 ± 2.8 MPa and 46.1 ± 3.6 MPa. On the other hand, composite materials with 0.50 wt.% and 3.00 wt.% of MWCNT, respectively, showed compressive modulus of 1,299.3 ± 39.5 MPa and 1,003.0 ± 51.1 MPa and compressive strength of 51.1 ± 1.0 MPa and 36.0 ± 0.6 MPa.

The Izod impact resistance was significantly higher for PA12-MWCNT than for PA12-GNP materials, despite the decrease in relation to the reference value of 5.1 ± 0.3 kJ/m^2 recorded in PA12 test specimens (Figure 10). In materials incorporating MWCNT, an average of 4.5 kJ/m^2 was obtained without significant variation between experiments. In turn, it was observed that there was a decrease in the impact resistance of PA12-GNP materials with the increasing amount of incorporation, from 2.5 ± 0.2 kJ/m^2 with 0.50 wt.% to 1.7 ± 0.2 kJ/m^2 with 3.00 wt.%.

It is known that the establishment of a uniform and homogeneous interaction of the reinforcements with the matrix is an essential condition to ensure the development of new materials for SLS with improved macro-scale properties (Mármol *et al.*, 2021). The aforementioned reduction in mechanical properties therefore suggests that the MWCNT and GNP may not be properly dispersed and distributed in the PA12 matrix. In fact, this is the main challenge in using these solutions due to the strong van der Waals forces and hydrophobic–hydrophilic interactions established between these reinforcements and polymers, such as PA12 (Madhad *et al.*, 2021).

3.5 Electrical properties

The results of surface resistance and electrical conductivity of composite materials incorporating MWCNT and GNP are shown in Figure 11.

With the incorporation of MWCNT and GNP until 3.00 wt.%, it was observed that there was a significant decrease in the surface resistance and an increase in the electrical conductivity

Figure 6 DSC thermograms of PA12, PA12-MWCNT and PA12-GNP materials

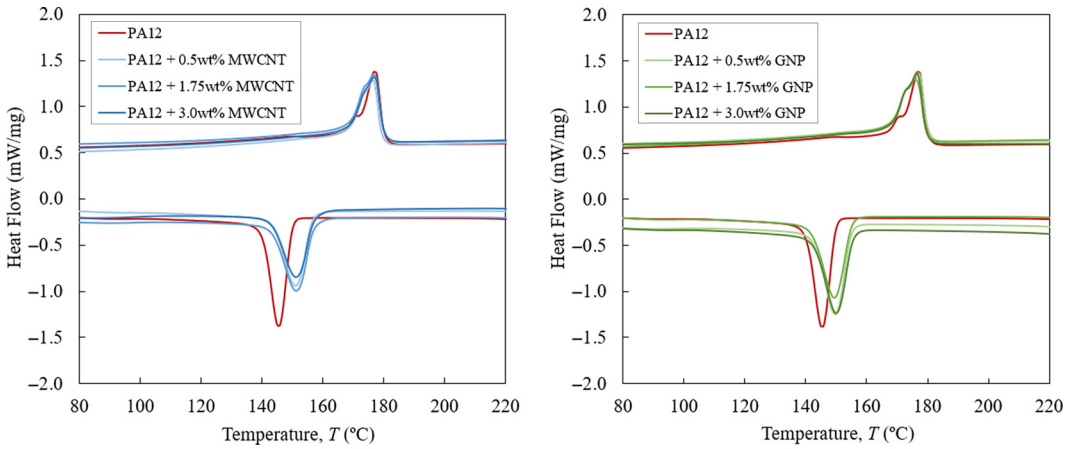

Source: Figure by authors

Figure 7 Thermal processing window of PA12, PA12-MWCNT and PA12-GNP materials

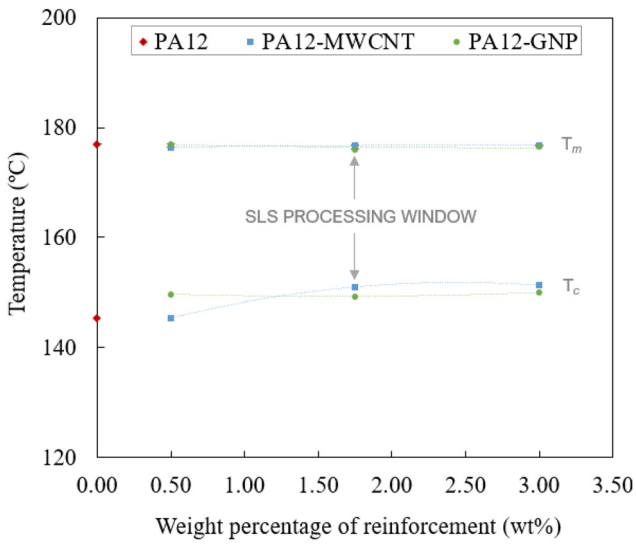

Source: Figure by authors

in relation to the polymer matrix. In both electrical parameters, MWCNT-based materials better-performed composites incorporating GNP. This may indicate that the long tubular structure of the MWCNT acts as a bridge between the carbon particles and the polymer, which is favourable for the creation of an effective conductive path in the materials, improving their electrical performance (Sanivada *et al.*, 2022). With regard to electrical surface resistance, values between 10^{10}–10^{3} Ω and 10^{9}–10^{4} Ω were, respectively, obtained in composite materials incorporating MWCNT and GNP in weight percentages between 0.50 wt.% and 3.00 wt.%. According to IEC 61340-5-1, composite materials incorporating 1.75 wt.% of GNP reached the electrostatic-dissipative range (i.e. $10^{5} \leq$ surface resistance $> 10^{11}$ Ω), proving its suitability for applications where it is necessary to ensure protection against electrostatic fields (e.g. manufacturing of enclosures or jigs for the automotive electronics industry) (Silva *et al.*, 2020). In both materials, the electrical conductivity gradually increased to 10^{-6} S/cm, surpassing the insulating range of the base polymeric matrix (Le *et al.*, 2017). This demonstrates that these carbon-based reinforcements can effectively be used to enhance the electrical properties of polymers with low percentages of incorporating (Sanivada *et al.*, 2022).

3.6 Morphological properties

Understanding the influence of the morphology on the aforementioned thermal, mechanical and electrical properties is of key importance for the successful development and production of composite materials by SLS. The analysis performed with an ultra-high-resolution microscope revealed significant differences in the cross-section of the test specimens produced with PA12-MWCNT and PA12-GNP materials with regard to the content of porosity and interparticle adhesion, compared to the reference condition of PA12 (Figure 12).

Agglomerates of MWCNT were extensively observed in the cross-section of test specimens produced with such composite materials (Figure 13). This is a consequence of the strong interactions and van der Waals forces established between the nanotubes, which were not efficiently counteracted by the mechanical mixing process. These effects became more evident with the increasing amount of MWCNT, as observed and analysed in a previous work (Lopes *et al.*, 2022a).

With the increasing percentage of incorporation of GNP from 0.50 wt.% to 3.00 wt.%, the cross-section of the test specimens was significantly modified, in particular from 0.50 wt.% to 1.75 wt.% (Figure 14).

At higher magnification, unsintered powder particles were clearly distinguished in the cross-section of the test specimens, suggesting that GNP acted as an inhibitor to the flow and consolidation of the polymer powder particles. As the amount of GNP increased to 3.00 wt.%, the surface area of polymer material available to establish a quality interparticle coalescence decreased. This impaired the definition of a strong, uniform and homogeneous cross-section (Figure 15).

Regardless of the carbon-based reinforcement, the microheterogeneities developed during the mixing and laser-sintering processing were responsible for the reduction in

Figure 8 Tensile elastic modulus (left) and tensile strength (right) of PA12, PA12-MWCNT and PA12-GNP materials processed by SLS

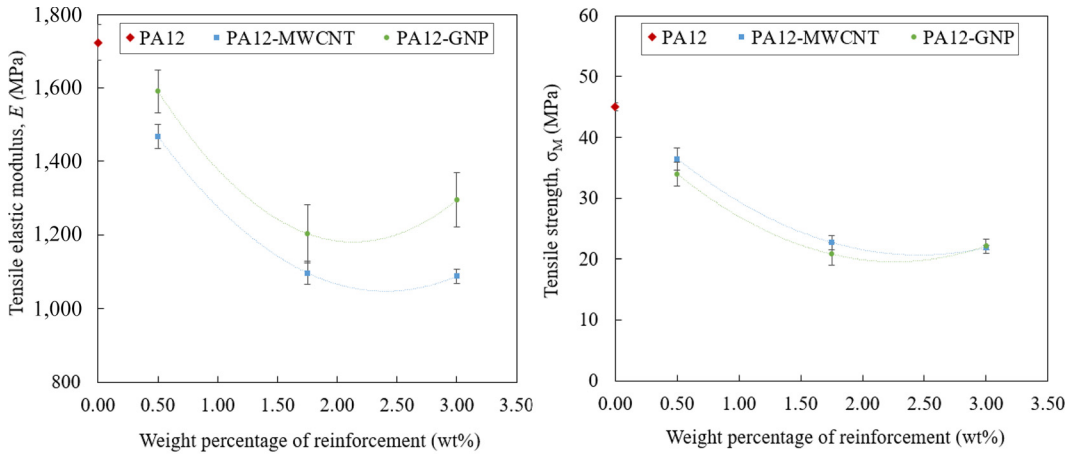

Source: Figure by authors

Figure 9 Compressive elastic modulus (left) and compressive strength (right) of PA12, PA12-MWCNT and PA12-GNP materials processed by SLS

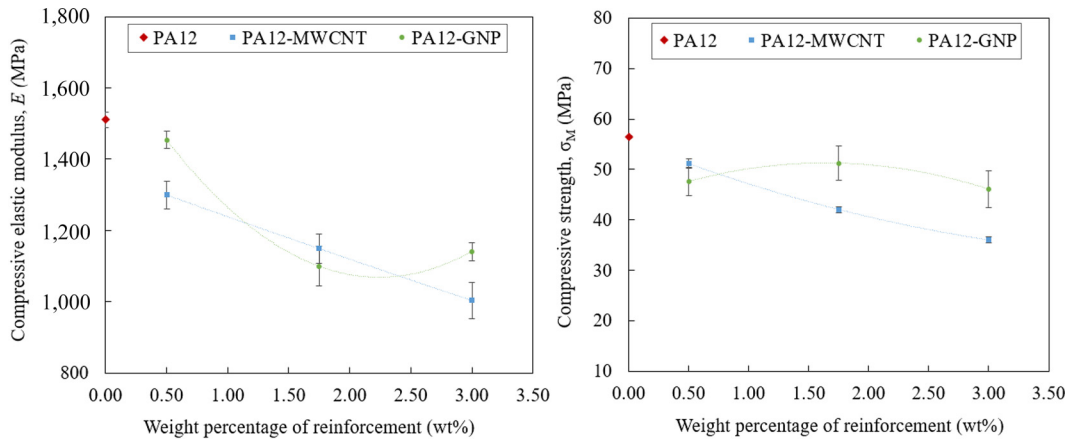

Source: Figure by authors

mechanical properties. Despite the weak dispersion that was developed, a great distribution of the particles was observed all over the cross-section of the test specimens (Figure 14), which may explain the creation of a conductive path able to reduce the electrical surface resistance of the parts, enhancing its electrical conductivity. This agrees with results from literature reporting that agglomerates of GNP may improve the electrical properties of the material in which they are incorporated (Sanivada *et al.*, 2022).

4. Conclusions

This research presents an analysis of the laser-sintering processing of polymer-based composite materials incorporating MWCNT and GNP and its influence on the thermal, mechanical, electrical and morphological properties of the parts produced.

The results first revealed that the selection of appropriate preparation methods is essential to obtain a uniform dispersion and distribution of the reinforcements in the matrix and, therefore, to create a composite material with homogeneous microstructure and thus improved macro-scale properties. In terms of processing, it was verified that composite materials incorporating these carbon-based reinforcements require lower energy density compared to the matrix due to their high thermal conductivity and enhanced ability for laser absorption. This was ensured by defining appropriate values of laser power, scan speed, hatch distance and layer thickness in each building job. The results obtained from the characterization tests revealed that, for same weight percentages of incorporation and conditions of preparation and processing, PA12-MWCNT materials allow the production of parts with higher tensile strength, impact resistance and electrical conductivity, with easier processability and lower costs compared to PA12-GNP materials. In turn, parts with greater surface quality, higher tensile elastic modulus and compressive strength were obtained with the incorporation of GNP into the PA12. Based on the intrinsic characteristics of each carbon allotrope and its different potential to influence the properties of polymers, parts with different mechanical properties and various levels of electrical

Figure 10 IZOD impact resistance of PA12, PA12-MWCNT and PA12-GNP materials processed by SLS

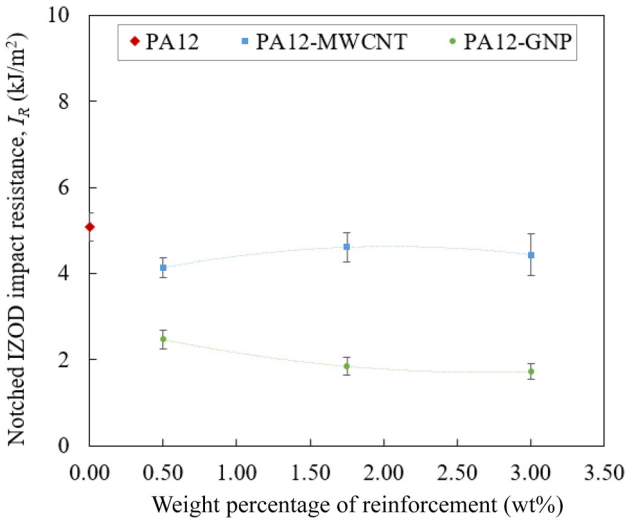

Source: Figure by authors

surface resistance and conductivity were obtained in this work. With the increasing amount of incorporation of MWCNT and GNP, the mechanical properties decreased due to the non-uniform stress distribution caused by the heterogeneous dispersion and distribution of the reinforcements in the mixture. In turn, the agglomerates distributed all over the cross-section of the parts allowed the creation of an electrically conductive path that reduced the electrical surface resistance of the parts produced until minimum values of $\sim 10^3\ \Omega$.

By exploring the development of new composites, this work aims to help broaden the materials portfolio for SLS and, ultimately, enable the use of laser-sintered parts in advanced applications where conventional materials do not meet specifications. In future work, advanced morphological characterization tests (e.g. EDX mapping, TEM) will be considered to analyse the raw materials and the prepared mixtures, aiming to understand their influence on the properties of the parts produced. Multi-step preparation methods will be studied to improve the adhesion between the polymer matrix and the reinforcements, enhancing the mechanical strength of the parts. Rheological properties may also be considered to analyse the flowability of the materials, depending on the typology of

Figure 11 Surface resistance (left) and electrical conductivity (right) of PA12, PA12-MWCNT and PA12-GNP materials processed by SLS

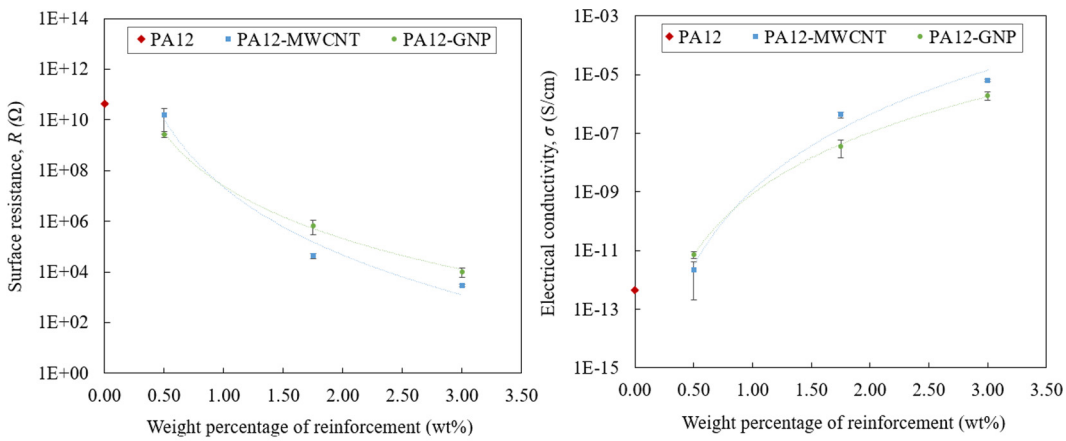

Source: Figure by authors

Figure 12 Cross-section of neat-PA12 (left) and PA12 incorporating 3.00 wt.% of MWCNT (middle) and) 3.00 wt.% of GNP (right) processed by SLS

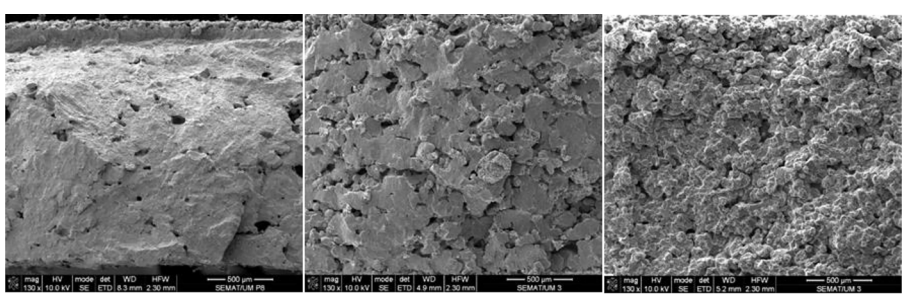

Source: Figure by authors

Figure 13 Cross-section of PA12 incorporating 3.00 wt.% of MWCNT processed by SLS at low (left) and high (right) magnification

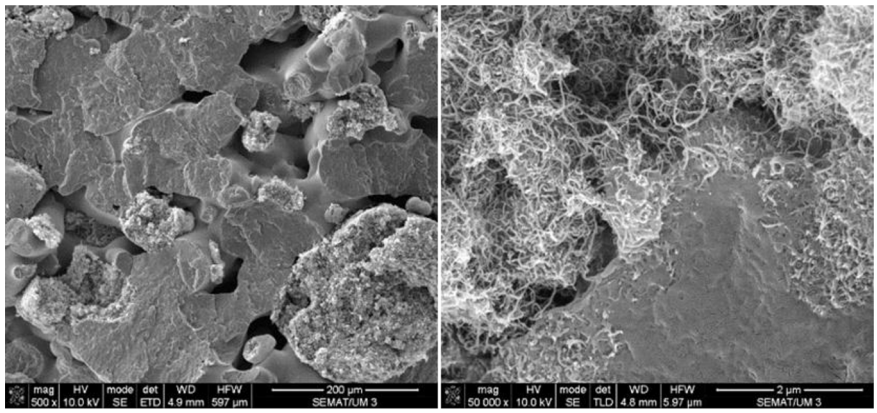

Source: Figure by authors

Figure 14 Cross-section of PA12 incorporating 0.50 wt.% (left), 1.75 wt.% (middle) and 3.00 wt.% (right) of GNP processed by SLS

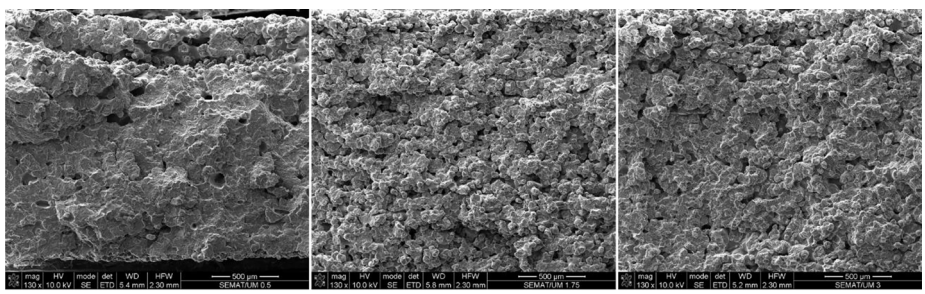

Source: Figure by authors

Figure 15 Cross-section of PA12 incorporating 3.00 wt.% of GNP processed by SLS at low (left) and high (right) magnification

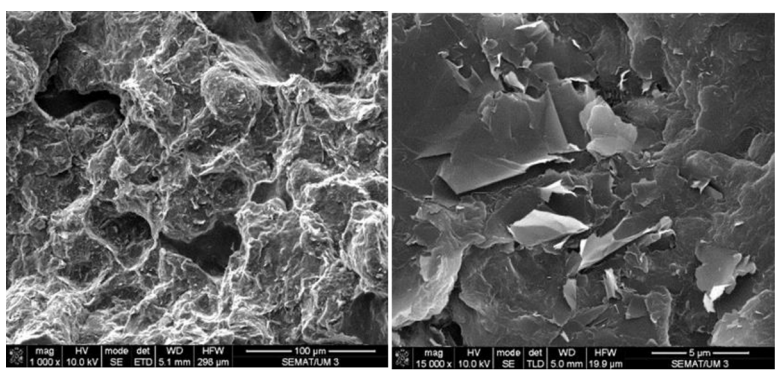

Source: Figure by authors

the reinforcement and amount of incorporation. Further investigation will also consider the fabrication of a case-study to validate all these findings in real conditions of implementation.

References

Asadi, A. and Kalaitzidou, K. (2018), "Process-structure-property relationship in polymer nanocomposites", in Marotti de Sciarra, F. and Russo, P. (Eds), *Experimental Characterization, Predictive Mechanical and Thermal Modeling of Nanostructures and Their Polymer Composites*, William Andrew, pp. 25-100, doi: 10.1016/B978-0-323-48061-1.00002-6.

ASTM (2012), "ASTM F2792 12a – standard terminology for additive manufacturing technologies".

Bai, J., Goodridge, R.D., Hague, R.J.M. and Song, M. (2013), "Improving the mechanical properties of laser-sintered

polyamide 12 through incorporation of carbon nanotubes", *Polymer Engineering & Science*, Vol. 53 No. 9, pp. 1937-1946.

Bai, J., Goodridge, R.D., Hague, R.J.M., Song, M. and Okamoto, M. (2014), "Influence of carbon nanotubes on the rheology and dynamic mechanical properties of polyamide-12 for laser sintering", *Polymer Testing*, Vol. 36, pp. 95-100.

Bai, J., Goodridge, R.D., Yuan, S., Zhou, K., Chua, C.K. and Wei, J. (2015), "Thermal influence of CNT on the polyamide 12 nanocomposite for selective laser sintering", *Molecules*, Vol. 20 No. 10, pp. 19041-19050.

Czelusniak, T. and Amorim, F.L. (2020), "Influence of energy density on selective laser sintering of carbon fiber-reinforced PA12", *The International Journal of Advanced Manufacturing Technology*, Vol. 111 Nos 7/8, pp. 2361-2376.

De Leon, A.C., Rodier, B.J., Bajamundi, C., Espera, A., Wei, P., Kwon, J.G., Williams, J., Ilijasic, F., Advincula, R.C. and Pentzer, E. (2018), "Plastic metal-free electric motor by 3D printing of graphene-polyamide powder", *ACS Applied Energy Materials*, Vol. 1 No. 4, pp. 1726-1733.

Eshraghi, S., Karevan, M., Kalaitzidou, K. and Das, S. (2013), "Processing and properties of electrically conductive nanocomposites based on polyamide-12 filled with exfoliated graphite nanoplatelets prepared by selective laser sintering", *International Journal of Precision Engineering and Manufacturing*, Vol. 14 No. 11, pp. 1947-1951.

Ferreira, T. (2013), *Microinjection Moulding of Polymeric Composites with Functionalized Carbon Nanotubes*, University of Minhoavailable at: https://repositorium.sdum.uminho.pt/handle/1822/35669?mode=full.

Francis, V. and Jain, P.K. (2015), "Advances in nanocomposite materials for additive manufacturing", *International Journal of Rapid Manufacturing*, Vol. 5 Nos 3/4, pp. 215-233.

Hong, R., Zhao, Z., Leng, J., Wu, J. and Zhang, J. (2019), "Two-step approach based on selective laser sintering for high performance carbon black/polyamide 12 composite with 3D segregated conductive network", *Composites Part B: Engineering*, Vol. 176, p. 107214.

Kharisov, B.I. and Kharissova, O.V. (2019), *Carbon Allotropes: Metal-Complex Chemistry, Properties and Applications*, 1st ed., Springer International Publishing, doi: 10.1007/978-3-030-03505-1.

Le, T.H., Kim, Y. and Yoon, H. (2017), "Electrical and electrochemical properties of conducting polymers", *Polymers*, Vol. 9 No. 12, p. 150.

Lopes, A.C., Sampaio, A.M. and Pontes, A.J. (2022a), "Composite materials with MWCNT processed by selective laser sintering for electrostatic discharge applications", *Polymer Testing*, Vol. 114, p. 107711.

Lopes, A.C., Sampaio, A.M. and Pontes, A.J. (2022b), "The influence of the energy density on dimensional, geometric, mechanical and morphological properties of SLS parts produced with single and multiple exposure types", *Progress in Additive Manufacturing*, Vol. 7 No. 4, pp. 683-698.

Madhad, H.V., Mishra, N.S., Patel, S.B., Panchal, S.S., Gandhi, R.A. and Vasava, D.V. (2021), "Graphene/graphene nanoplatelets reinforced polyamide nanocomposites: a review", *High Performance Polymers*, Vol. 33 No. 9, pp. 981-997.

Ma-Hock, L., Strauss, V., Treumann, S., Küttler, K., Wohlleben, W., Hofmann, T., Gröters, S., Wiench, K., van Ravenzwaay, B. and Landsiedel, R. (2013), "Comparative inhalation toxicity of multi-wall carbon nanotubes, graphene, graphite nanoplatelets and low surface carbon black", *Particle and Fibre Toxicology*, Vol. 10 No. 1, pp. 1-20.

Makuch, A., Trzaska, M., Skalski, K. and Bajkowski, M. (2015), "PA-G composite powder for innovative additive techniques", *Composites Theory and Practice*, Vol. 15 No. 3, pp. 152-157.

MarketWatch (2022), "Selective laser sintering market demand 2022", available at: www.marketwatch.com/press-release/selective-laser-sintering-market-demand-2022-in-depth-analysis-of-industry-growth-revenue-global-size-share-statistics-top-players-strategies-future-scope-investment-opportunities-and-outlook-analysis-2028-2022-04 (accessed 20 June 2022).

Mármol, G., Sanivada, U.K. and Fangueiro, R. (2021), "Effect of GNPs on the piezoresistive, electrical and mechanical properties of PHA and PLA films", *Fibers*, Vol. 9 No. 12, pp. 1-18.

Paggi, R.A., Beal, V.E. and Salmoria, G.V. (2013), "Process optimization for PA12/MWCNT nanocomposite manufacturing by selective laser sintering", *The International Journal of Advanced Manufacturing Technology*, Vol. 66 Nos 9/12, pp. 1977-1985.

Parandoush, P. and Lin, D. (2017), "A review on additive manufacturing of polymer-fiber composites", *Composite Structures*, Vol. 182, pp. 36-53.

Razeghi, M. (2019), '*The Carbon Atom', in The Mystery of Carbon – An Introduction to Carbon Materials*, Institute of Physics Publishing, pp. 1-12, available at: https://iopscience.iop.org/book/mono/978-0-7503-1182-3/chapter/bk978-0-7503-1182-3ch1.

Salmoria, G.V., Paggi, R.A. and Beal, V.E. (2017), "Graded composites of polyamide/carbon nanotubes prepared by laser sintering", *Lasers in Manufacturing and Materials Processing*, Vol. 4 No. 1, pp. 36-44.

Salmoria, G.V., Paggi, R.A., Lago, A. and Beal, V.E. (2011), "Microstructural and mechanical characterization of PA12/MWCNTs nanocomposite manufactured by selective laser sintering", *Polymer Testing*, Vol. 30 No. 6, pp. 611-615.

Sanivada, U.K., Esteves, D., Arruda, L.M., Silva, C.A., Moreira, I.P. and Fangueiro, R. (2022), "Joule-heating effect of thin films with carbon-based nanomaterials", *Materials*, Vol. 15 No. 12, p. 4323.

Silva, C.S., Lima, A., Rodrigues, S.J.F., Gonçalves, L.F.F.F., Sampaio, Á.M., Oliveira, L., Fernandes, A. and Pontes, A.J. (2020), "Development of functionalised foam for electrostatic discharge applications", *Plastics, Rubber and Composites*, Vol. 49 No. 10, pp. 470-478.

Tian, X., Peng, G., Yan, M., He, S. and Yao, R. (2018), "Process prediction of selective laser sintering based on heat transfer analysis for polyamide composite powders", *International Journal of Heat and Mass Transfer*, Vol. 120, pp. 379-386.

Tong, Q., Xue, K., Wang, T. and Yao, S. (2020), "Laser sintering and invalidating composite scan for improving tensile strength and accuracy of SLS parts", *Journal of Manufacturing Processes*, Vol. 56, pp. 1-11.

Wu, H., Fahy, W.P., Kim, S., Kim, H., Zhao, N., Pilato, L., Kafi, A., Bateman, S. and Koo, J.H. (2020), "Recent developments in polymers/polymer nanocomposites for additive manufacturing", *Progress in Materials Science*, Vol. 111, p. 100638.

Yuan, S., Shen, F., Chua, C.K. and Zhou, K. (2019), "Polymeric composites for powder-based additive manufacturing: materials and applications", *Progress in Polymer Science*, Vol. 91, pp. 141-168.

Yuan, S., Bai, J., Chua, C.K., Wei, J. and Zhou, K. (2016), "Material evaluation and process optimization of CNT-coated polymer powders for selective laser sintering", *Polymers*, Vol. 8 No. 10, p. 370.

Yuan, S., Zheng, Y., Chua, C.K., Yan, Q. and Zhou, K. (2018), "Electrical and thermal conductivities of MWCNT/polymer composites fabricated by selective laser sintering", *Composites Part A: Applied Science and Manufacturing*, Vol. 105, pp. 203-213.

Zakaria, M.R., Abdul Kudus, M.H., Md. Akil, H. and Mohd Thirmizir, M.Z. (2017), "Comparative study of graphene nanoparticle and multiwall carbon nanotube filled epoxy nanocomposites based on mechanical, thermal and dielectric properties", *Composites Part B: Engineering*, Vol. 119, pp. 57-66.

Corresponding author

Ana C. Lopes can be contacted at: acarinalopes@dep.uminho.pt